ELSEVIER

Journal of Alloys and Compounds 229 (1995) 268–273

Journal of ALLOYS AND COMPOUNDS

Electrochemical and surface properties of the $Zr(V_{0.2}Mn_{0.2}Ni_{0.6})_{2.4}$ alloy electrode

Xueping Gao, Deying Song, Yunshi Zhang, Zuoxiang Zhou, Wei Zhang, Mei Wang, Panwen Shen

Institute of New Energy Material Chemistry, Nankai University, Tianjin 300071, People's Republic of China

Received 18 January 1995; in final form 26 April 1995

Abstract

In order to further improve the electrocatalytic activity and activation behaviour of the $Zr(V_{0.2}Mn_{0.2}Ni_{0.6})_{2.4}$ alloy electrode, the alloy powder surface was treated by HF acid solution and the electrochemical properties of both electrodes were measured. It was found that the surface treatment by HF acid solution was significantly effective on improving the electrocatalytic activity and activation behaviour of the alloy electrode by means of electrochemical impedance spectroscopy. The surface properties of the untreated and treated alloy powders were investigated by scanning electron spectroscopy and X-ray photoelectron spectroscopy. The effected factors on the electrocatalytic activity such as the chemical state and composition of alloy powder surfaces before and after treatment by HF acid solution were discussed. Additionally, the crystallographic characterization and the hydrogen storage performance of the alloy were also examined.

Keywords: Electrochemistry; Surface properties; Electrocatalytic activity; $Zr(V_{0.2}Mn_{0.2}Ni_{0.6})_{2.4}$ alloy

1. Introduction

Laves-phase alloy hydrides are expected to act as new negative materials for reversible metal hydride batteries with a high electrochemical capacity and a long cycle life. However, it is known that they have the disadvantage of requiring many charge–discharge cycles for activation. In particular, the Laves-phase alloy electrode was disappointing in electrocatalytic activity compared with the $MmNi_5$-based alloy electrode. Furthermore, the bulk diffusion rate of hydrogen in the alloy is fast and the primary obstacle in achieving high-rate discharge is related to the surface electrocatalytic activity of the Laves-phase alloy electrode. Therefore, the improvement of the electrocatalytic activity of the Laves-phase alloy electrode was absolutely necessary for electrochemical application. Yan et al. [1] studied the F-treatment effect on a ZrTiVNi alloy and found the activation and kinetic properties of the alloy electrode were remarkably improved. Zuttel et al.'s [2] investigated results also confirmed this effect for the $Zr(V_{0.25}Ni_{0.75})_2$ alloy electrode.

In this work, we have focused on the $Zr(V_{0.2}Mn_{0.2}Ni_{0.6})_{2.4}$ alloy with a C15-type Laves phase structure. After the treatment by HF acid solution, the electrocatalytic activity and activation behaviour of the alloy electrode were considerably improved. The electrocatalytic activity was generally characterized by electrochemical reaction resistance [3]. The chemical state and composition of the alloy powder were analyzed using X-ray photoelectron spectroscopy (XPS). X-ray diffraction (XRD) was also employed to characterize the alloy structure properties. Additionally, the hydrogen-storage performance of the alloy was investigated.

2. Experimental details

The $Zr(V_{0.2}Mn_{0.2}Ni_{0.6})_{2.4}$ alloy (about 10 g) was prepared by arc melting the constituent elements under an argon atmosphere on a water-cooled copper plate. The alloy was crushed and ground mechanically to particle size without annealing. The alloy and its hydride were then analyzed by powder diffraction. The crystallographic parameters of the alloy and its hydride were calculated. The hydrogen-storage performance of the alloy was measured by determination

SSDI 0925-8388(95)01704-6

of the desorption pressure–composition–temperature (PCT) isotherms. The alloy powder was treated by HF acid solution (pH = 1.5–2.5) for 15 min and rinsed with distilled water and then dried. The chemical state and composition of the alloy powder surface untreated and treated by HF acid solution were measured by means of XPS in a PHI-5300 ESCA spectrometer using Mg Kα radiation of energy 1253.6 eV. The surface morphologies of the alloy powders untreated and treated by HF acid solution were measured by scanning electron microscopy (SEM).

For the electrochemical measurements approximately 0.50 g of the alloy powder were mixed with carbonyl nickel powder(0.15 g) and polyvinyl alcohol (PVA) (0.005 g) and then compacted into a porous nickel substrate (20 mm × 20 mm). After that, the substrate was dried and then pressed.

The properties of a negative electrode were examined using a sintered nickel electrode with a large capacity as the counterelectrode and a Hg/HgO (5 M KOH) electrode as the reference electrode. The discharge capacity was measured under a current density of 50 mA g^{-1} at ambient temperature and the cut-off potential for each discharge was set to be − 0.740 V. After about 15 charge–discharge cycles of activation, the electrochemical impedance spectra were carried out under open-circuit conditions using a Solartron 1250 frequency response analyzer and a TD3690 potentiostat. The impedance spectra of the electrodes were recorded from 10 KHz to 10 mHz and at 5 mV of the amplitude of perturbation for the different depths of discharge (DODs).

3. Results

3.1. Structure and PCT curves

The $Zr(V_{0.2}Mn_{0.2}Ni_{0.6})_{2.4}$ alloy and its hydride were analyzed by XRD (Fig. 1). It was found that the alloy has mainly a cubic C15-type Laves phase structure. The residual phases were a hexagonal C14-type Laves phase and a Zr_9Ni_{11} phase. After hydrogenation the lattice parameter (a) increased from 7.0355 Å to 7.4292 Å, but the crystal structure did not change. Besides, the alloy hydride became fine grains in terms of pattern peak intensity and half-peak width. Moreover, the expansion of the lattice volume was determined to be 17.7% ($\Delta V/V$) for H/M = 0.75 at 0.1 MPa. The typical pressure–composition desorption isotherms of the $Zr(V_{0.2}Mn_{0.2}Ni_{0.6})_{2.4}$ alloy are illustrated in Fig. 2. It was shown that the alloy has a wider plateau region and a flatter plateau pressure compared with the Zr–V–Ni alloy [4]. The enthalpy change (ΔH) and entropy change (ΔS) were evaluated to be − 39.9 KJ (mol H_2)$^{-1}$ and − 125.7 KJ (mol H_2)$^{-1}$ for H/M = 0.55 from the PCT curves by the Van't Hoff equation $\ln(P_e/P_0) = \Delta H/RT - \Delta S/R$.

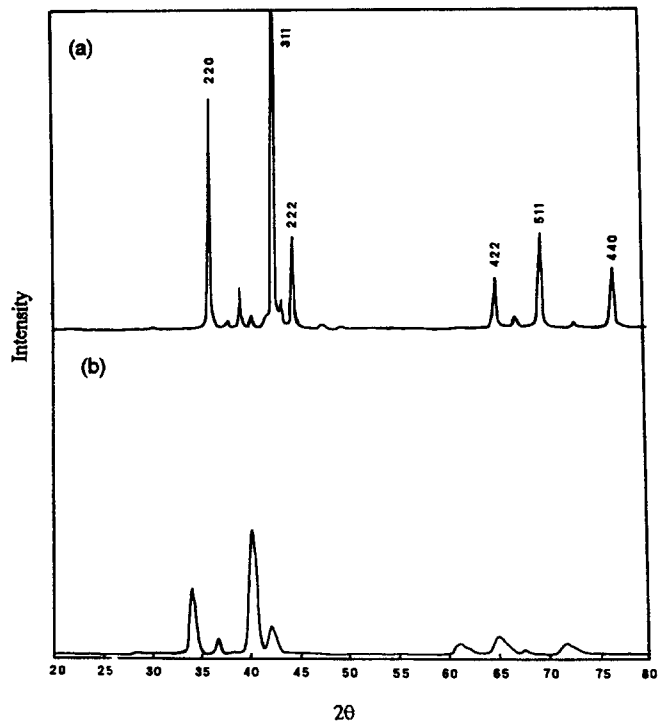

Fig. 1. X-ray diffraction patterns for the $Zr(V_{0.2}Mn_{0.2}Ni_{0.6})_{2.4}$ alloy (a) and its hydride (b).

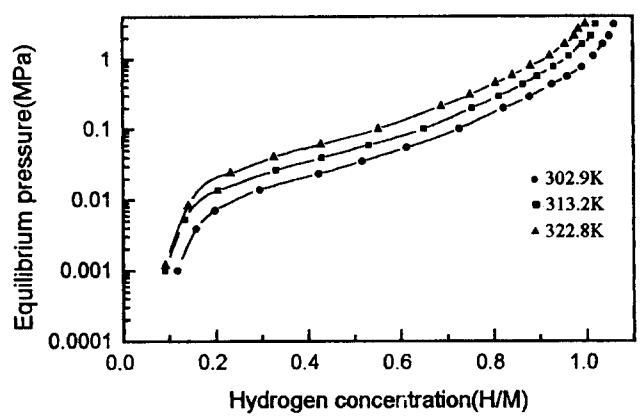

Fig. 2. Pressure–composition–temperature isotherms of desorption for the $Zr(V_{0.2}Mn_{0.2}Ni_{0.6})_{2.4}$ alloy.

3.2. Activation and electrocatalytic activity

The discharge capacities of the $Zr(V_{0.2}Mn_{0.2}Ni_{0.6})_{2.4}$ alloys untreated and treated by HF acid solution at room temperature in every cycle were measured under a constant discharge current of 50 mA g^{-1} and are shown in Fig. 3. It was found that the untreated alloy electrode showed a smaller initial capacity (Fig. 3(a)). However, the treated alloy electrode showed a higher initial discharge capacity (Fig. 3(b)) and an excellent activation behaviour.

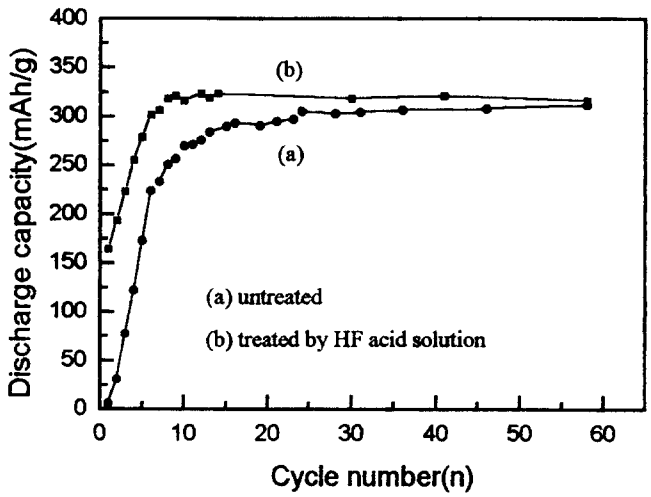

Fig. 3. Discharge capacities as a function of cycle number for the untreated (a) and treated (b) $Zr(V_{0.2}Mn_{0.2}Ni_{0.6})_{2.4}$ alloy electrodes under a discharge current of 50 mA g^{-1}.

The impedance spectra of the untreated and treated $Zr(V_{0.2}Mn_{0.2}Ni_{0.6})_{2.4}$ alloy electrodes from 10 KHz to 10 mHz at different depths of discharge (DODs) are shown in Fig. 4. The Cole–Cole plots almost consisted of two obvious comparable semicircles. The smaller semicircle in the high-frequency region was probably a typical double-layer capacitance and hardly changed. The big semicircle in the low-frequency region, which exhibited remarkable dependence on hydrogen content (or DOD), was attributed to an electrochemical reaction [3]. The reaction resistances from the semicircle in the low-frequency region were calculated by fitting program. The DOD dependence of the reaction resistance for the untreated and treated alloy electrodes is illustrated in Fig. 5. It was shown through the experiment data that the reaction resistances were increased with decreasing hydrogen content for both electrodes. In particular, the reaction resistances of the treated alloy electrode has been obviously decreased compared with that of the untreated alloy electrode at the same depth of discharge. Thus, the electrocatalytic activity of the treated alloy electrode was remarkably improved. Besides, as can be seen from Fig. 4, the electrochemical reaction for both electrodes was mainly under surface charge transfer control. In a discharge depth of 109% for the treated alloy electrode (Fig. 4(b)), there was an obvious slope related to Warburg impedance in the Cole–Cole plot. This result meant that when the hydrogen content decreased, the rate-determining step was changed from the surface charge transfer to a mixed process of the surface charge transfer and the hydrogen diffusion in the alloy bulk. Therefore, it can be concluded that the HF acid solution treatment was effective on the improvement of the activation behaviour and electrocatalytic activity of the alloy electrode.

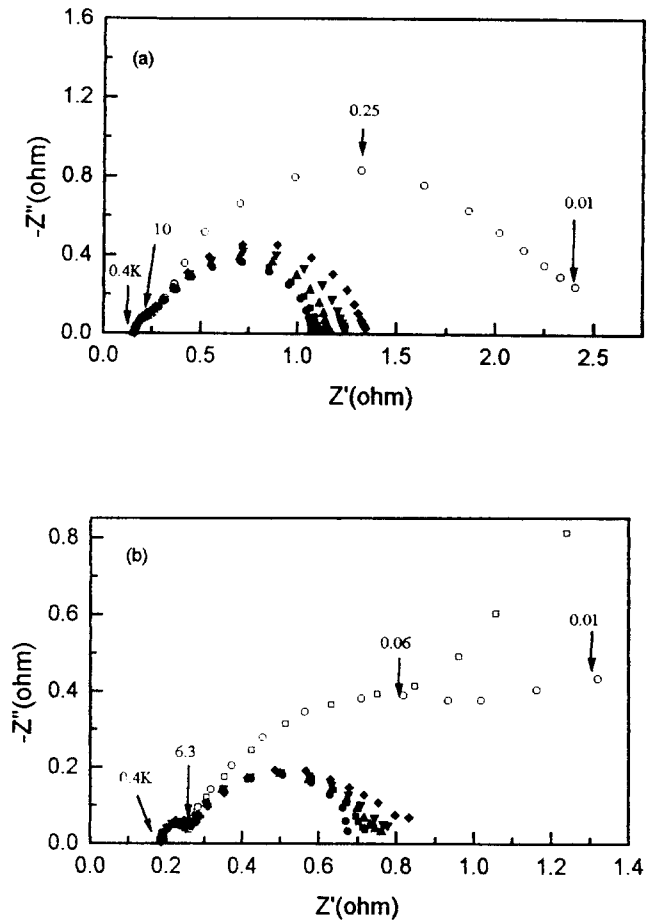

Fig. 4. Cole–Cole plots for the untreated (a) and treated (b) $Zr(V_{0.2}Mn_{0.2}Ni_{0.6})_{2.4}$ alloy at different DOD%: (a) ●, 0%; ■, 20%; ▲, 40%; ▼, 60%; ♦, 80%; ○, 100%; (b)●, 0%; ■, 20%; ▲, 40%; ▼, 60%; ♦, 80%; ○, 100%; □, 109%.

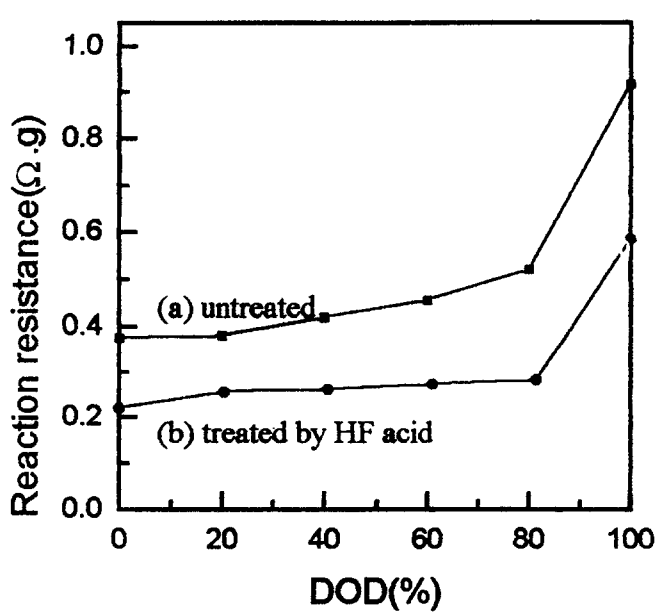

Fig. 5. DOD dependences of the reaction resistances for the untreated (a) and treated (b) $Zr(V_{0.2}Mn_{0.2}Ni_{0.6})_{2.4}$ alloy electrodes.

3.3. Surface state

The electrochemical reaction process always takes place on the alloy/solution interface. Therefore, it is important to obtain information about the alloy surface state. The physical, chemical and composition changes at the surface occurring during HF acid solution treatment of the $Zr(V_{0.2}Mn_{0.2}Ni_{0.6})_{2.4}$ alloy powder were analyzed by SEM and XPS techniques. Fig. 6 presents the SEM micrographs for the alloy powder surfaces of the $Zr(V_{0.2}Mn_{0.2}Ni_{0.6})_{2.4}$ alloy before and after treatment by HF acid solution. The observation shown was that the surface of the untreated alloy powder was smoother, but that of the treated alloy powder was rougher and was full of cracks owing to dissolution of some constituent element oxides into HF acid solution. Within a crack, there was a new created surface. BET measurement indicated that the specific surface area was increased from 0.10 $m^2\ g^{-1}$ to 0.28 $m^2\ g^{-1}$ after the treatment by HF acid solution.

To assess the elemental distribution and chemical state on the alloy surface, XPS was conducted on the untreated and treated alloy powder samples. The composition changes on the alloy surface were significant after the treatment by HF acid solution (Fig. 7). There was a stronger segregation of zirconium and manganese on the untreated alloy powder surface due to the lower surface energy of zirconium and manganese [4]. The nickel content on the alloy surface was lower compared with the bulk composition. The alloy treated by HF acid solution showed that the nickel was enriched and the other constituent elements were depleted by comparison. The chemical states of Zr, V, Mn and Ni were examined by determining the binding energy. The core level spectra revealed that the zirconium, vanadium and manganese on the alloy surface were completely oxidized to ZrO_2 (181.8 eV), V_2O_3 (516.7 eV) and MnO (641.2 eV), respectively. The nickel was partially oxidized and existed as NiO (855.7 eV) and in the metallic state (852.8 eV) (Fig. 8). After the treatment by HF acid solution, the alloy surface was almost covered with oxides of the constituent elements except nickel owing to exposure to air in the experiment.

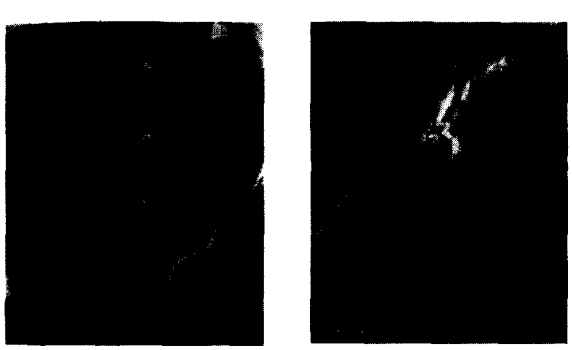

(a) (b)

Fig. 6. SEM micrographs × 6000 for untreated (a) and treated (b) $Zr(V_{0.2}Mn_{0.2}Ni_{0.6})_{2.4}$ alloy powder.

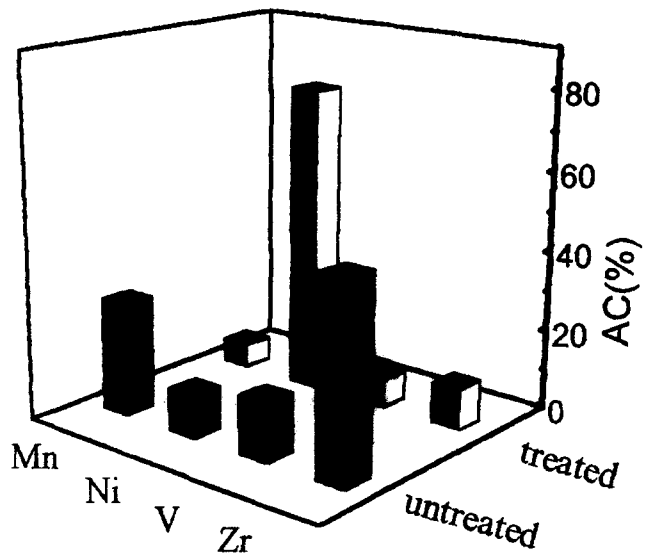

Fig. 7. The surface atomic concentration for the untreated and treated by HF acid solution $Zr(V_{0.2}Mn_{0.2}Ni_{0.6})_{2.4}$ alloy.

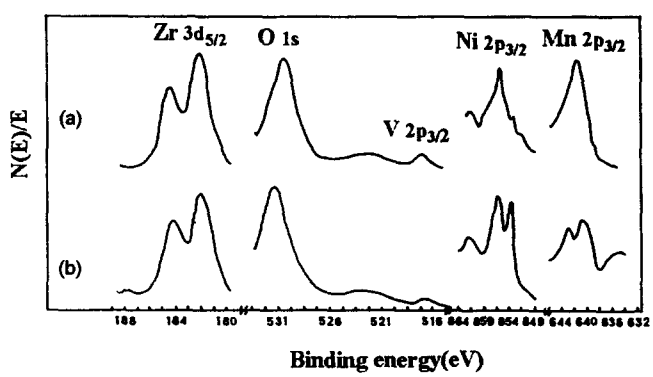

Fig. 8. Zr3d, V2p, Ni2p, Mn2p and O1s core level spectra for the untreated (a) and treated (b) $Zr(V_{0.2}Mn_{0.2}Ni_{0.6})_{2.4}$ alloy by HF acid solution.

4. Discussion

Generally speaking, the high rate dischargeability of the hydrogen storage electrode is controlled by many factors such as the surface electrocatalytic activity, hydrogen diffusion rate in alloy bulk, and hydrogen plateau pressure in PCT curves, and so on [5]. In accordance with the results described in the above section, it was found that the $Zr(V_{0.2}Mn_{0.2}Ni_{0.6})_{2.4}$ alloy has a wider plateau region and an available plateau pressure which were beneficial to electrochemical application.

In comparison with the $MmNi_5$-based hydrogen-

storage electrode, the Laves-phase hydrogen-storage electrode was poor in the electrocatalytic activity [3]. Among varieties of contributed factors to the electrocatalytic activity, the effect of the surface state was obvious, because the electrochemical reaction always occurs on the alloy surface. The untreated alloy powder surface was almost coated by a dense and passive ZrO_2 layer which is a barrier to the dissociation of water and the penetration of hydrogen. During cycling in the KOH solution, vanadium oxide on the alloy surface dissolved in an alkaline solution to form a VO_2^- ion. The metal vanadium on the new surface further corroded forming vanadium oxide and dissolved owing to creation of microporosity. Therefore, the electrode was activated after some cycles. However, the electrocatalytic activity of the alloy electrode was still poor due to the presence of more zirconium oxide on the surface, which is hardly dissolved in an alkaline solution. After the treatment by HF acid solution, the specific surface area of the alloy powder increased on account of roughness, cracks and pores. The improvement of the specific surface area was considered beneficial to good performance in decreasing electrode polarization. In addition, the metal zirconium and ZrO_2 are more easily dissolved in HF acid solution to further form stable complex ions such as ZrF_6^{2-}, ZrF_7^{3-} and ZrF_8^{4-}, etc., because the Zr^{4+} ion is relatively large, highly charged, and spherical with no partly filled shell to give it stereochemical preferences [6]. The metallic vanadium and manganese and their oxides also dissolved in HF acid solution to form VF_3 and MnF_2, but the metallic nickel hardly dissolved by comparison. Consequently, the treatment procedure made the alloy surface elements selectively dissolve into the HF acid solution and provided a Ni-rich alloy surface. Although partial nickel in the outer surface existed as NiO owing to exposure to air during experiment, the $Ni(OH)_2$ (in an alkaline solution) can be reduced to metallic nickel during charging. ($Ni(OH)_2 + 2e \Leftrightarrow Ni + 2OH^-$ at -0.818 V vs. Hg/HgO/OH^- electrode [7]). The metallic nickel on the alloy surface could be believed to be the metallic clusters of nickel atoms or the Raney-type nickel [8], which has a high specific surface area (geometric factor) and a lower activation energy for the dissociation of water (energy factor). Therefore, the electrocatalytic activity of the treated alloy electrode was excellent.

It was easily found that the electrochemical reaction resistances for both untreated and treated alloy electrodes progressively increased with decreasing hydrogen concentration. However, the electrochemical reaction resistances were significantly increased in the discharge end stage as a result of decreasing hydrogen concentration (near the α phase from the PCT curves) and oxidation of the outer surface nickel (the discharge end potential was -0.740 V and the steady-state potential was about -0.830 V).

The previous investigated results on Zr-based Laves-phase hydrogen-storage electrodes has indicated that the hydrogen diffusion rate in the alloy bulk was fast and the surface charge transfer was the rate-determining step [3,5,9]. It was evident from the foregoing results that there was a slope related to the Warburg impedance in the low-frequency region for the discharge end stage of the treated alloy electrode. It was concluded that the hydrogen diffusion rate in the bulk decreased with decreasing hydrogen concentration and the rate-determining step was a mixed process of the surface charge transfer and the hydrogen diffusion in the alloy bulk.

5. Conclusion

The poor activation behaviour and electrocatalytic activity of the untreated $Zr(V_{0.2}Mn_{0.2}Ni_{0.6})_{2.4}$ alloy electrode were probably caused by the presence of a dense and passive ZrO_2 layer, which is a barrier to the dissociation of water and the penetration of hydrogen, After the treatment by HF acid solution, the activation behaviour and electrocatalytic activity of the alloy electrode was significantly improved. Especially, the rate-determining step of the electrode reaction was changed from the surface charge transfer to a mixed process of the surface charge transfer and the hydrogen diffusion in the alloy bulk at the discharge end stage. The reason was caused firstly by increasing the specific surface area, and secondly by transferring the surface from the Zr-rich layer to the Ni-rich layer. The nickel on the outer surface can be believed to be the metallic clusters of nickel atoms or the Raney-type nickel, which is of benefit to improving electrocatalytic activity.

Acknowledgments

This work was supported by the National Advanced Material Committee of China (NAMCC). The authors wish to express their thanks to Mr. H.B. Yang for EIS analyses.

References

[1] D.Y. Yan, Y.M. Sun and S.Suda, *Int. Symp. Metal–Hydrogen Systems Fundamentals and Applications, Japan, November 6, 1994*,, this issue.

[2] A. Zuttel, F. Meli and L. Schlapbach, *J. Alloys Comp., 209* (1994) 99.

[3] N. Kuriyama, T. Sakai, H. Miyamura I. Uehara and H. Ishikawa, *J. Alloys Comp., 202* (1993) 183.
[4] A.R. Miedema, *Z. Metall., 69* (1978) 287.
[5] X.P. Gao, D.Y. Song, Y.S. Zhang, Z.X. Zhuo, W.Zhang, P.W. Shen and M. Wang, *Int. Symp. on Metal–Hydrogen Systems Fundamentals and Applications, Japan, November 6, 1994*, this issue.
[6] F.A. Cotton and G. Wilkinson, *Advanced Inorganic Chemistry*, Wiley, 1972, 3rd edn., p. 822.
[7] John A. Dean (ed.), *Lange's Handbook of Chemistry*, McGraw–Hill, 1985, 3rd edn., pp. 6–13.
[8] K. Machida, M. Enyo, I. Toyoshima, K. Miyahara, K. Kai and K. Suzuki, *Bull. Chem. Soc. Jpn., 56* (1983) 3393.
[9] M.A. Fetcenko, S. Venkatesan, K.C. Hong and B. Beichman, *Power Sources, 12* (1989) 411.